

MIT Open Access Articles

Roles for the transcription elongation factor NusA in both DNA repair and damage tolerance pathways in Escherichia coli

The MIT Faculty has made this article openly available. **Please share** how this access benefits you. Your story matters.

Citation: Cohen, S. E., C. A. Lewis, R. A. Mooney, M. A. Kohanski, J. J. Collins, R. Landick, and G. C. Walker. "Roles for the Transcription Elongation Factor NusA in Both DNA Repair and Damage Tolerance Pathways in Escherichia Coli." *Proceedings of the National Academy of Sciences* 107, no. 35 (August 31, 2010): 15517–15522.

As Published: <http://dx.doi.org/10.1073/pnas.1005203107>

Publisher: National Academy of Sciences (U.S.)

Persistent URL: <http://hdl.handle.net/1721.1/85183>

Version: Final published version: final published article, as it appeared in a journal, conference proceedings, or other formally published context

Terms of Use: Article is made available in accordance with the publisher's policy and may be subject to US copyright law. Please refer to the publisher's site for terms of use.



Roles for the transcription elongation factor NusA in both DNA repair and damage tolerance pathways in *Escherichia coli*

Susan E. Cohen^a, Cindi A. Lewis^{a,1}, Rachel A. Mooney^b, Michael A. Kohanski^{c,d}, James J. Collins^{c,d}, Robert Landick^{b,e}, and Graham C. Walker^{a,2}

^aDepartment of Biology, Massachusetts Institute of Technology, Cambridge, MA 02139; ^bDepartment of Biochemistry and ^cDepartment of Bacteriology, University of Wisconsin, Madison, WI 53706; ^dHoward Hughes Medical Institute, Department of Biomedical Engineering, Center for BioDynamics, and Center for Advanced Biotechnology, Boston University, Boston, MA 02215; and ^eBoston University School of Medicine, Boston, MA 02118

Edited by Jeffrey W. Roberts, Cornell University, Ithaca, NY, and approved July 13, 2010 (received for review April 16, 2010)

We report observations suggesting that the transcription elongation factor NusA promotes a previously unrecognized class of transcription-coupled repair (TCR) in addition to its previously proposed role in recruiting translesion synthesis (TLS) DNA polymerases to gaps encountered during transcription. Earlier, we reported that NusA physically and genetically interacts with the TLS DNA polymerase DinB (DNA pol IV). We find that *Escherichia coli nusA11(ts)* mutant strains, at the permissive temperature, are highly sensitive to nitrofurazone (NFZ) and 4-nitroquinolone-1-oxide but not to UV radiation. Gene expression profiling suggests that this sensitivity is unlikely to be due to an indirect effect on gene expression affecting a known DNA repair or damage tolerance pathway. We demonstrate that an *N*²-furfuryl-dG (*N*²-f-dG) lesion, a structural analog of the principal lesion generated by NFZ, blocks transcription by *E. coli* RNA polymerase (RNAP) when present in the transcribed strand, but not when present in the nontranscribed strand. Our genetic analysis suggests that NusA participates in a nucleotide excision repair (NER)-dependent process to promote NFZ resistance. We provide evidence that transcription plays a role in the repair of NFZ-induced lesions through the isolation of RNAP mutants that display altered ability to survive NFZ exposure. We propose that NusA participates in an alternative class of TCR involved in the identification and removal of a class of lesion, such as the *N*²-f-dG lesion, which are accurately and efficiently bypassed by DinB in addition to recruiting DinB for TLS at gaps encountered by RNAP.

excision repair | RNA polymerase | translesion synthesis | Mfd | transcription-coupled

The process of nucleotide excision repair (NER) acts to remove a wide variety of DNA lesions and in *Escherichia coli* is mediated through the concerted action of the *uvrA*, *uvrB*, and *uvrC* gene products (1). The process of transcription-coupled repair (TCR) targets NER to actively transcribed genes, resulting in preferential repair of the transcribed strand relative to the nontranscribed strand (2–4). In *E. coli*, the *mfd*⁺ gene product couples the process of NER to transcription, and has been shown to be responsible for the strand specific repair of UV-induced lesions (5–7).

We have recently reported that the highly conserved TLS polymerase DinB (DNA pol IV), a member of the class of specialized DNA polymerases that can replicate damaged DNA, interacts physically and genetically with the transcription elongation factor NusA (8, 9). Δ *dinB* strains are sensitive to DNA-damaging agents, nitrofurazone (NFZ) and 4-nitroquinolone-1-oxide (4-NQO), and DinB preferentially and accurately bypasses a structural analog of the major NFZ-induced *N*²-dG lesion as well as certain other *N*²-dG adducts (10–13). NusA is an essential, multidomain protein that functions in both termination and antitermination of transcription, and is associated with the RNA polymerase (RNAP) throughout the elongation and termination phases of transcription (14–22). We have proposed a model of transcription-coupled translesion synthesis (TC-TLS) in which NusA recruits DinB to sites of RNAP stalled by a gap in the transcribed strand that is opposite a lesion in

the nontranscribed strand so DinB can fill in the gap to provide a template for transcription (8).

Here, we report our striking observations that *nusA* mutants are highly sensitive to NFZ and that this sensitivity is unlikely to be due to an indirect effect of gene expression changes. We present evidence that NusA participates in an NER-dependent process as well as a DinB-dependent process to promote survival after challenge with NFZ. Moreover, we provide additional *in vivo* evidence that transcription plays a role in the repair of NFZ-induced lesions. Together, our results suggest that NusA, in addition to its roles in transcription elongation and termination, is important for coordinating the cellular responses to DNA damage by coupling the processes of NER and TLS to transcription. Our results suggest an additional reason for the conservation of *nusA*⁺ throughout bacteria and archaea.

Results

***nusA* Mutant Strains Are Sensitive to DNA-Damaging Agents.** To further investigate the role for NusA in DNA repair/damage tolerance pathways, we explored the possibility that *nusA* mutants might render cells sensitive to exposure to DNA-damaging agents. Strikingly, we observed that at the permissive temperature (30 °C), *nusA11(ts)* strains are specifically sensitive to the DNA-damaging agents NFZ and 4-NQO, but not to UV, methyl methanesulfonate (MMS) (Fig. 1), ethyl methanesulfonate (EMS), or hydrogen peroxide. This sensitivity to NFZ and 4-NQO can be complemented by providing *nusA*⁺ *in trans* at the permissive temperature (Fig. S1A and B). The greater sensitivity of a *nusA11* mutant strain compared with that of a Δ *dinB* strain implies that NusA participates in a *dinB*-independent, as well as a *dinB*-dependent, role in promoting survival after exposure to NFZ or 4-NQO.

The fact that the *nusA11* mutation does not sensitize cells to UV, MMS, EMS, or hydrogen peroxide indicates that the expression of genes involved in the various DNA repair and damage tolerance pathways that enable cells to cope with lesions induced by these agents—nucleotide excision repair, base excision repair, recombinational repair, and *umuDC* mediated TLS (reviewed in ref. 1)—is not perturbed. Additionally, at the permissive temperature, *nusA11* mutant strains display wild-type levels of UV-induced mutagenesis (9), suggesting that SOS induction and DNA pol V (UmuD₂C) are operating normally. Collectively, these data suggest that the sensitivity to NFZ and 4-NQO observed in

Author contributions: S.E.C., R.A.M., R.L., and G.C.W. designed research; S.E.C., C.A.L., and R.A.M. performed research; M.A.K. and J.J.C. contributed new reagents/analytic tools; S.E.C., R.A.M., R.L., and G.C.W. analyzed data; and S.E.C., R.L., and G.C.W. wrote the paper.

The authors declare no conflict of interest.

This article is a PNAS Direct Submission.

See Commentary on page 15314.

¹Present address: Genomic Medicine Institute, Cleveland Clinic, Cleveland, OH 44195.

²To whom correspondence should be addressed. E-mail: gwalker@mit.edu.

This article contains supporting information online at www.pnas.org/lookup/suppl/doi:10.1073/pnas.1005203107/-DCSupplemental.

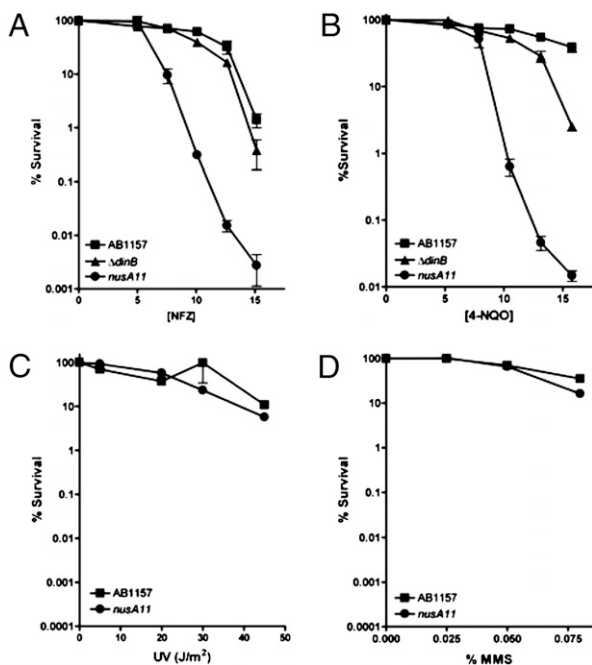


Fig. 1. *nusA11* mutants are specifically sensitive to NFZ and 4-NQO. (A) Percent survival of strains treated with 0–15 μ M NFZ. All graphs in this figure's experiments were performed at the permissive temperature (30 $^{\circ}$ C), and error bars represent the SD determined from at least three independent cultures. (B) Percent survival of strains treated with 0–17.5 μ M 4-NQO. At 30 $^{\circ}$ C the sensitivity of the Δ *dinB* strain to NFZ and 4-NQO is less than the degree of sensitivity observed at 37 $^{\circ}$ C (10). (C) Percent survival of strains irradiated with 0–45 J/m² UV. (D) Percent survival of strains treated with 0–0.08% MMS.

a *nusA11* mutant strain is not likely due to an indirect effect of gene expression on a DNA repair or damage tolerance process. We also performed microarray analyses to assess the genome-wide changes in gene expression that occur in a *nusA11* background at the permissive temperature. We did not observe changes in the expression of any genes known to be involved in DNA repair or damage tolerance, but rather differential expression of genes whose products are involved in a variety of aspects of cellular metabolism (Table S1 and Table S2). These findings motivated us to investigate the alternative hypothesis that NusA might play a hitherto unsuspected role in DNA repair.

The striking recessive sensitivity of *nusA11* mutant strains to NFZ at the permissive temperature indicates that it is a partial loss-of-function mutation. The analysis of a strain completely lacking *nusA* is not feasible in standard *E. coli* genetic backgrounds, because *nusA* is essential for viability. However, it is possible in a specialized genetic background lacking horizontally transferred DNA (23, 24). In such a strain (MDS42), we observe that both *nusA11* and Δ *nusA* mutations result in sensitivity to NFZ and 4-NQO (Fig. 2A and D). However, the complete loss of *nusA* additionally results in sensitivity to UV and MMS (Fig. 2), supporting the notion that the *nusA11* allele is a partial loss-of-function mutant. Providing *nusA*⁺ *in trans* complements the NFZ, UV, and MMS sensitivity as well as the growth defect of a Δ *nusA* strain (Fig. S1C). Microarray analysis of the *nusA* deletion strain (23) did not reveal any statistically significant changes in the expression of genes whose products have been implicated in DNA repair. Although we cannot unambiguously rule out the possibility that the increased sensitivity to killing by these DNA-damaging agents is due to an effect on gene expression, these data are consistent with the hypothesis that *nusA*⁺ participates directly in a process that promotes cellular survival after challenge with DNA damage.

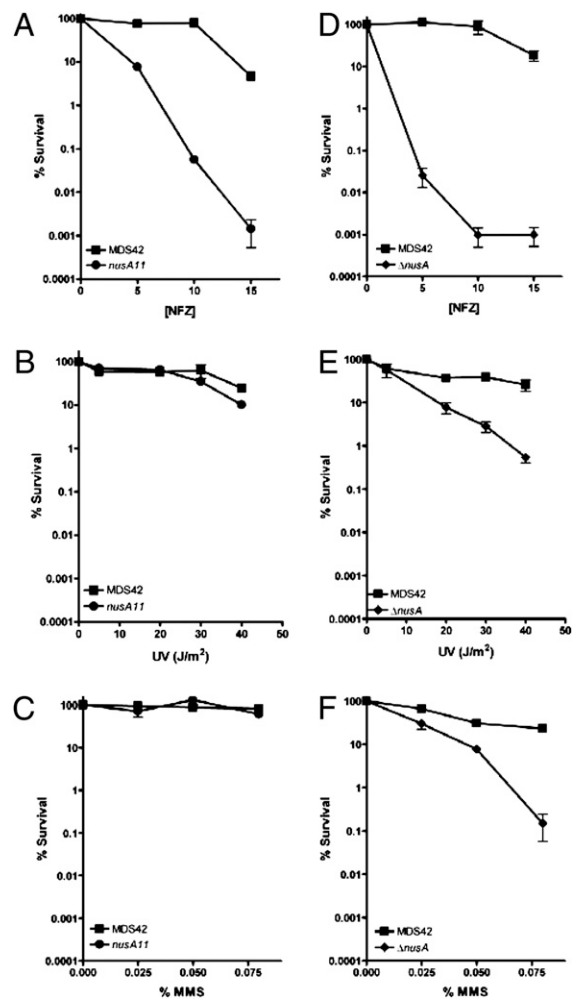


Fig. 2. Comparison of *nusA11* and Δ *nusA* mutations in MDS42. (A–C) Percent survival of strains treated with the DNA-damaging agents NFZ (μ M), UV, and MMS, respectively, at 30 $^{\circ}$ C. For all graphs in this figure, error bars represent the SD determined from at least three independent cultures. (D–F) Percent survival of strains treated with the DNA-damaging agents NFZ (μ M), UV, and MMS, respectively, at 37 $^{\circ}$ C.

***N*²-furfuryl-dG Lesion Blocks Transcription by *E. coli* RNAP.** If the specific sensitivity of *nusA11* mutant strains after exposure to NFZ and 4-NQO were due to a failure to repair a specific class of lesion introduced by these agents, what could these lesions be? A possible answer is suggested by our previous observations that DinB carries out preferential and accurate TLS over *N*²-furfuryl-dG (*N*²-f-dG), a mimic of the major adduct formed by NFZ (10, 25). Given that DinB is present in considerable excess over the replicative DNA polymerase in both SOS-uninduced cells (250 DinB/10–20 pol III) and SOS-induced cells (2,500 DinB/10–20 pol III) (26, 27), it seems likely that *N*²-f-dG lesions with properties similar to *N*²-f-dG would be readily bypassed by DinB, resulting in their continued presence in the genome where they could potentially hinder transcription.

To test the hypothesis that this type of lesion would obstruct transcription, we monitored *E. coli* RNAPs ability to use a template containing the *N*²-f-dG lesion *in vitro*. The presence of an *N*²-f-dG lesion on the transcribed strand completely blocked transcription (Fig. 3), whereas the presence of the same lesion on the nontranscribed strand had little effect on transcription (Fig. S24). Generation of a 3' dCMP-terminated transcript allowed us to map the position of the transcript generated when *N*²-f-dG is present on the transcribed strand, showing that transcription is stalled four nucleotides (ntd) upstream of the lesion (Fig. S2B).

Stalling of RNAP at such a lesion in the transcribed strand could be a detection mechanism that then allows repair proteins to subsequently be recruited.

We also monitored the ability of RNAP to bypass template strand gaps, which we propose stall transcription in our model of TC-TLS. We observed that *E. coli* RNAP is able to bypass a 1-ntd gap, with similar efficiencies to those previously published (~45% bypass) (28). However, unlike T7 RNAP (28, 29), transcription by *E. coli* RNAP is unable to bypass a larger, 14-ntd gap (~2% bypass) (Fig. 3). Even with prolonged incubation time, RNAP is not capable of bypassing either the N^2 -f-dG adduct or 14-ntd gapped templates (Fig. S3). Moreover, addition of purified NusA or NusA11 to the reactions did not directly alter RNAPs ability to transcribe through these modified templates (Fig. S4). This observation indicates that NusA does not act by modulating RNAPs ability to carry out transcription over a lesion or a gap in the transcribed strand but instead suggests that NusA might play a role in the recruitment of factors, such as

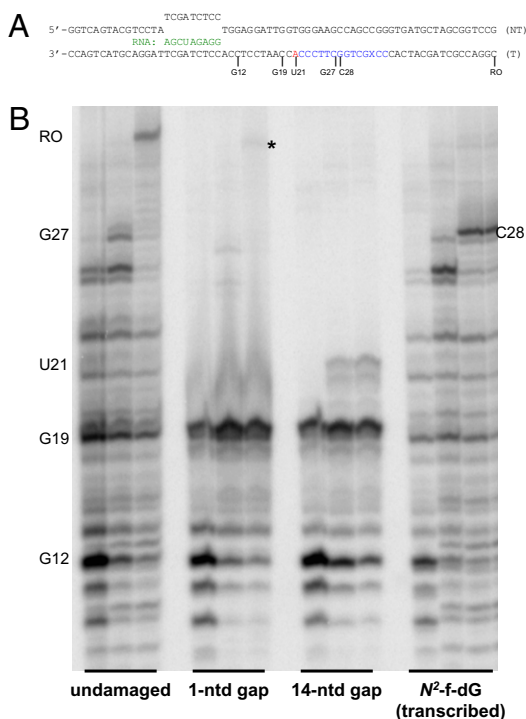


Fig. 3. *E. coli* RNA polymerase does not bypass template strand gaps or a N^2 -f-dG lesion. (A) Schematic of experimental design. Three oligonucleotides, one containing the N^2 -f-dG lesion or an undamaged proxy, are ligated together to generate the transcribed strand (T) using the nontranscribed strand (NT) as a scaffold. A 9-ntd noncomplementary region between the (T) DNA and (NT)DNA allows for the annealing of an RNA primer (green) to initiate transcription. For each nucleic acid scaffold, purified RNAP, UTP, and [32 P] α GTP are added to radiolabel the RNA transcript and extend to G12. Because of the limiting ATP left over from the ligation reaction, we observe the addition of several nucleotides to the transcript (first lane of B). The addition of excess cold ATP, UTP, and GTP extends the RNA to the G27 position (second lane of B). Addition of CTP allows for transcription through the lesion or proxy to the end of the scaffold in the full-length/undamaged template (third lane of B; band labeled RO). "X" indicates the site of N^2 -furfuryl-dG lesion or proxy dG, nucleotide colored in red represents the position of the 1-ntd gap, and nucleotides colored in blue represent the position of the 14-ntd gap. Positions labeled in B represent the extension of RNA primer as marked, underneath the templating base, in schematic. (B) For each template (labeled at bottom), the first lane is the transcription reaction after addition of UTP, [32 P]GTP, and limiting ATP to allow labeling and extension to G12; the second lane is the reaction after the addition of excess ATP, UTP, and GTP; and the third lane is the reaction after the addition of CTP. All lanes represent 1-min time points. The asterisk represents the product formed on the 1-ntd gap.

DNA repair systems or DinB for TLS, to sites of RNAP stalled by an N^2 -dG lesion or by a gap.

Identification of a NusA-Dependent, *uvr*-Dependent Process for NFZ Resistance. Two prior observations led us to consider the possibility that NusA might play a role in the recruitment of nucleotide excision repair (NER) machinery to an RNAP that has been stalled by an NFZ-induced lesion. First, a high-throughput protein interaction screen identified NusA as an interaction partner of UvrA (30), which we have confirmed by far Western blotting (Fig. 4A). Additionally, Δ *uvrA* strains are sensitive to NFZ, and *uvr*-dependent NER is the predominant mechanism for processing NFZ-induced DNA damage in *E. coli* (31).

Epistasis analysis with respect to NFZ sensitivity of *nusA11* and Δ *uvrA* alleles revealed that Δ *uvrA* is largely epistatic to *nusA11* (Fig. 4B), suggesting that NusA plays a role in a UvrA-dependent process. Δ *uvrB* and Δ *uvrC* alleles are similarly epistatic to *nusA11* with respect to sensitivity to NFZ. Because NusA is a component of elongating RNA polymerases, it seems possible that the *uvr*-dependent process that the *nusA11* mutation might be affecting could be a type of transcription-coupled nucleotide excision repair of lesions introduced by NFZ. However, we observe an additive relationship for both NFZ and 4-NQO sensitivity with Δ *mfd* and *nusA11* alleles, implying that NusA and Mfd function in separate pathways (Fig. 4C), and suggesting the possibility that NusA is required for an alternative type of Mfd-independent transcription-coupled nucleotide excision repair. In contrast epistasis analysis with respect to UV sensitivity of Δ *nusA* and Δ *mfd* alleles revealed a synergistic relationship in which the double mutant was much more sensitive than either of the single mutants (Fig. 4D). This suggests that, in addition to any roles with Mfd in promoting TCR of UV-induced lesions, NusA additionally plays a role in more generally directing NER (Discussion).

RNA Polymerase Mutants Display an Altered Ability to Deal with NFZ.

To search for additional in vivo evidence that transcription might play a role in directing *uvr*-dependent NER of lesions introduced by NFZ, we screened the previously described plasmid-borne mutant libraries of *rpoB* (32), which encodes for the β catalytic subunit of RNAP, for the ability to cause either NFZ sensitivity (NFZ^S) or NFZ resistance (NFZ^R). We isolated three single mutants: the NFZ^S mutant *rpoB*(D185Y) and NFZ^R mutants *rpoB*(V287A) and *rpoB*(D320N). The NFZ^S mutant *rpoB*(D185Y) displayed a 10-fold sensitivity to NFZ compared with an *rpoB*⁺ plasmid control, whereas the NFZ^R mutants *rpoB*(V287A) and *rpoB*(D320N) displayed a 10-fold resistance (Fig. 4E).

We observed that, when expressed in a Δ *dinB* (Fig. S5B) or Δ *mfd* (Fig. 4F) background, these *rpoB* mutants displayed the same pattern of NFZ^S or NFZ^R, although the relative degree of NFZ^S or NFZ^R differs from that observed in a wild-type background, indicating that these gene products do not play a role in this phenomenon. Strikingly, when expressed in a *nusA11* background, this pattern was altered because these *rpoB* mutants had largely lost their ability to confer NFZ^S or NFZ^R (Fig. 4G and Fig. S5A). Similarly, in a Δ *uvrA* background, expression of these *rpoB* mutants also resulted in loss of the original pattern of relative sensitivity or resistance (Fig. 4H). These results indicate that the original pattern of NFZ sensitivity or resistance depends on *nusA*⁺ and *uvrA*⁺. The fact that mutating a core component of RNA polymerase affects the *nusA*-dependent, *uvr*-dependent process of NFZ resistance we have identified provides additional evidence that this process could be a previously unrecognized form of transcription-coupled repair that functions independently of Mfd.

Intriguingly, mapping these *rpoB* mutations on the crystal structure of *T. thermophilus* RNAP elongation complex (33) revealed that all three were located in the leading part of RNA polymerase that would first encounter a lesion in double-stranded DNA during the process of transcription (Fig. S5C). The crystal structure predicts that when RNAP stalls at the -4 position relative to the N^2 -f-dG lesion in the transcribed strand, the N^2 -f-dG

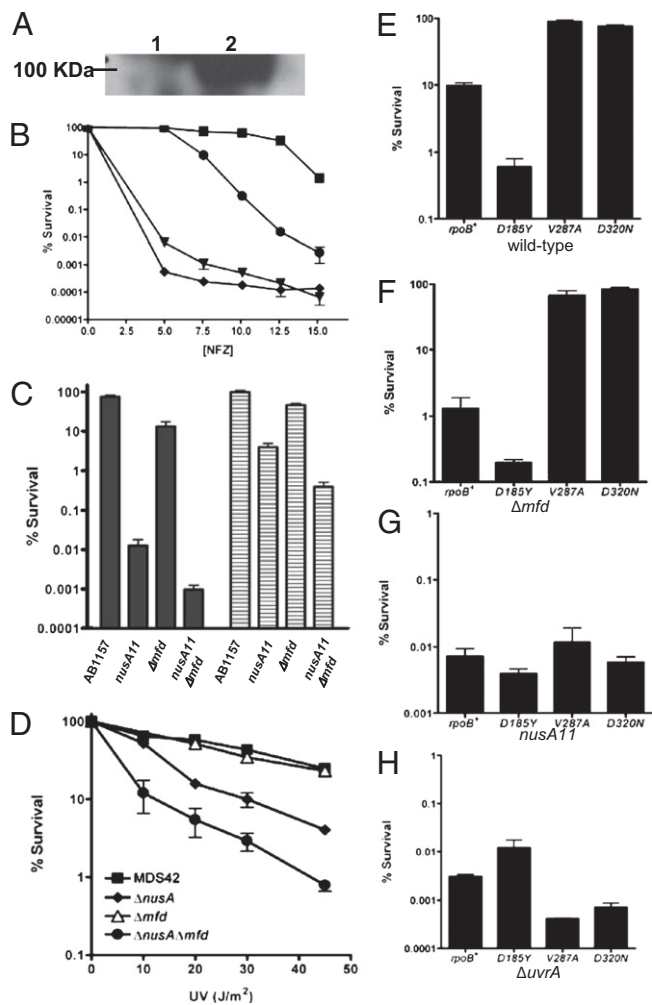


Fig. 4. Interactions with NER and a role for transcription. (A) Far-Western blot demonstrates that NusA interacts with UvrA. Cell lysates harboring the empty vector (lane 1) or overexpressing UvrA (lane 2) were separated by SDS/PAGE, transferred to a PVDF membrane, and incubated with purified NusA. α -NusA antibodies detected the binding of NusA to a 100-kDa migrating protein specifically in the UvrA (103 kDa) overexpressing lane. (B) Percent survival of strains treated with 0–15 μ M NFZ at 30 °C. Squares, wild type/AB1157; circles, *nusA11* (SEC164); inverted triangles, Δ *uvrA* (SEC 316); diamonds, *nusA11* Δ *uvrA* (SEC318). In this and all graphs in this figure, error bars represent the SD determined from at least three independent cultures. (C) *nusA11* and Δ *mfd* strains display an additive phenotype with respect to NFZ (filled bars) or 4-NQO (striped bars) sensitivity at 10 μ M at 30 °C. (D) Percent survival of strains, MDS42, Δ *nusA*, Δ *mfd* (SEC1629), and Δ *nusA* Δ *mfd* double mutants (SEC1276), to UV irradiation demonstrates that the Δ *nusA* Δ *mfd* double mutant is much more sensitive than either of the single mutants. (E) Sensitivity of *rpoB* mutants expressed in AB1157 to 10 μ M NFZ at 37 °C. (F) Sensitivity of *rpoB* mutants expressed in a Δ *mfd* background to 10 μ M NFZ at 37 °C. (G) Sensitivity of *rpoB* mutants expressed in a *nusA11* mutant background to 12.5 μ M NFZ at 30 °C. (H) Sensitivity of *rpoB* mutants expressed in a Δ *uvrA* background to 10 μ M NFZ at 37 °C. Despite differences in the survival of Δ *uvrA* strains expressing the *rpoB* variants, the ability of each *rpoB* mutant to confer NFZ^S or NFZ^R as observed in a *uvrA*⁺ strain background is lost.

adduct would be located in the minor groove of the dsDNA ahead of the transcription bubble.

Induction of DNA Damage in *nusA11*. To test whether the NusA-dependent repair process we had postulated is important for processing endogenous lesions, we examined whether untreated *nusA11* strains at the permissive temperature show indications that they have suffered DNA damage. We observed a 4-fold

increase of SOS induction (34) in exponential phase *nusA11* cells (0.8%) compared with 0.2% in wild-type cells (Fig. S6A–C) and a 25-fold increase in stationary-phase *nusA11* cells (~2.5%) compared with wild type (~0.1%) (Fig. 5A–C). As expected, *lexA* (Def) cells, lacking the LexA repressor, display SOS induction in 100% of cells in both exponential and stationary phase. Additionally, we observed that *nusA11* cells were somewhat elongated compared with *nusA*⁺ cells, with a smaller population displaying extreme filamentation, >30 times the size of *nusA*⁺ cells, specifically in stationary phase (Fig. S6D and E). The distribution of RecA-GFP foci of exponentially growing *nusA11* cells is similar to that of *nusA*⁺ cells (0–5 foci per cell) (35) (Fig. S6F–I). In contrast, in stationary-phase cells, grown at the permissive temperature, RecA-GFP foci are observed in ~2% of wild-type cells and ~19% of *nusA11* cells, 8.5-fold higher than *nusA*⁺ cells. If wild-type strains are irradiated with UV, all cells then have RecA-GFP foci (Fig. 5D–F).

Discussion

We propose that, in addition to its postulated role in TC-TLS (8), NusA plays a key role in a previously unrecognized pathway of transcription-coupled NER that is distinct from the well characterized Mfd-dependent pathway. This NusA-dependent transcription-coupled repair pathway (NusA-TCR) is important for the repair of a class of DNA lesion typified by the N²-f-dG adduct, a structural analog of the major NFZ-induced lesion. Such lesions could be considered “stealth lesions” in that they can be readily bypassed during DNA replication because of the high levels of DinB relative to the replicative DNA polymerase, but then absolutely block transcription when present in the transcribed strand. NusA-TCR would help prioritize the cell’s NER resources to maximally benefit transcription while also facilitating the recognition and repair of lesions that are otherwise more difficult to detect (Fig. 6). There are 20 molecules of UvrA/SOS-uninduced cell and 250 molecules of UvrA/SOS-induced cell (1), in many cases there would be more lesions than UvrA molecules.

We speculate that the RNAP β lobe, which contains the NFZ^S D185R substitution, may facilitate RNAP backtracking upon encountering a lesion or gap in the template DNA so as to expose downstream DNA. NER may then be recruited to the DNA via contacts to NusA and possibly to the lineage-specific insertion β i4 (36) in which the NFZ^R V287A and D320N substitutions are located. Precedence exists for RNAP backtracking to expose a downstream DNA priming site for DNA polymerases during M13 phage replication (37).

The apparent role of NusA in recruitment of NER machinery to damaged DNA raises an interesting structural question given the known interactions of NusA on the face of RNAP opposite to the downstream DNA entering an elongating complex. *E. coli* NusA contacts the RNAP α -subunit CTD via the C-terminal NusA acidic repeat domains (AR1 and AR2) (38) and contacts the RNA exit channel via its N-terminal domain (39, 40); these contacts position the S1 domain and G181 (*nusA11* is G181D) near the β 'dock, in which a suppressor of *nusA11* (*rpoC10*; E402K) has been mapped (22, 41). In contrast, the NFZ^S substitution in the β lobe, the NFZ^R substitutions in β i4, and the downstream DNA are ~150 Å from the RNA exit channel and ~125 Å from the position of α CTD attachment to RNAP via a flexible linker. Could NusA target NER over these distances? The combined length of the flexible α -subunit linker, the α CTD, and the NusA AR domains is at least 120 Å. Furthermore, the linearly arranged domains of NusA span >150 Å from N to C terminus. Because the NER machinery also must span some distance, it appears to be plausible that they could be recruited to the downstream side of RNAP by NusA tethered either to the α CTD via AR2 or to exiting RNA and the RNAP exit channel via the NusA NTD.

Although elegant biochemical studies of Mfd-dependent TCR have offered detailed insights into the mechanism by which it repairs UV-induced DNA damage (5–7), it is striking that, in contrast to mutation of the mammalian transcription-coupling repair factor (42, 43), Δ *mfd* mutants display only a modest in-

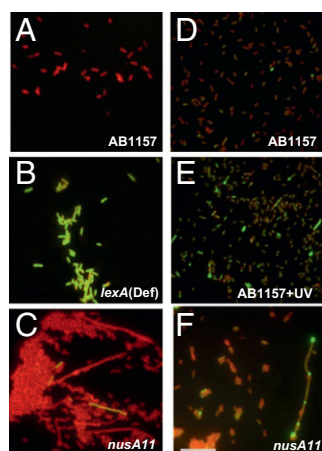


Fig. 5. *nusA11* cells display phenotypes of altered DNA processing in stationary phase. (A–C) Representative micrographs of stationary-phase wild-type (AB1157) (SEC677) (A), *lexA(Def)* (SEC678) (B), and *nusA11* cells (SEC679) (C). Number of cells counted (*n*) was 731 for wild type, 330 for *lexA(Def)*, and 402 for *nusA11*. Cell outlines (red) were visualized with the vital membrane stain FM4-64, and SOS induction was monitored from P_{sulA} -GFP fusion integrated at an ectopic locus on the chromosome (34) (green). (D–F) Representative micrographs of stationary-phase wild-type (AB1157) cells (*n* = 2,000) (D), wild-type (AB1157) cells irradiated with 25 J/m² UV and left to recover in the dark for 10 min (*n* = 509) (E), and stationary-phase *nusA11* cells (*n* = 362) (F). Cell outlines (red) were visualized with the vital membrane stain FM4-64, and RecA-GFP foci are shown in green. RecA-GFP translational fusion is chromosomally expressed from endogenous locus (35).

crease in sensitivity to UV (44). This has led to the inference that TCR is much less important in bacteria than eukaryotes. Our results suggest an alternative interpretation: TCR is as important in bacteria as it is in eukaryotes, but its importance has been underappreciated in the past because the existence of an alternative Mfd-independent pathway of TCR had not yet been recognized. Interestingly, the *N*²-f-dG lesion stalls transcription at the –4 position in contrast to UV lesions that enter the active site of the RNAP (45–48). These observations may suggest a possible explanation for why the *nusA11* mutation differentially affects TCR of the two classes of lesions.

The sensitivity of $\Delta nusA$ mutant strains to other agents such as UV and MMS suggests that NusA could also play a role in the transcription-coupled repair of lesions introduced by these agents as well. Our epistasis analysis does not exclude the possibility that NusA works in conjunction with Mfd to promote TCR of UV-induced lesions but does indicate that NusA plays a role in directing NER in a manner that is independent of Mfd. Interestingly, the sequenced genomes of several cancer cell lines have suggested the existence of an additional class of NER that is preferentially deployed to both transcribed and nontranscribed strands of genes compared with intergenic DNA (49, 50) or genes that are not expressed (51), which is of greater importance than strand-specific repair (50). Thus, it is possible that NusA-dependent NER is a variant of TCR that can remove lesions from both strands analogous to the system inferred to exist in mammalian cells (49–51).

Additionally, we observed that *nusA11* mutant strains display chronic partial SOS induction that is greater in stationary phase than during exponential growth and a striking increase in RecA-GFP foci particularly in stationary phase. The fact that these phenotypes, indicative of DNA damage, are observed without the addition of exogenous DNA-damaging agents implies that *nusA11* mutant cells cannot properly deal with endogenous DNA damage. What could account for these observations? First, a metabolite generated at higher levels in stationary-phase cells than in exponentially growing cells could be causing DNA damage that depends on *nusA*⁺ for repair. Secondly, it is possible that active replication during exponential growth may mask any defects in

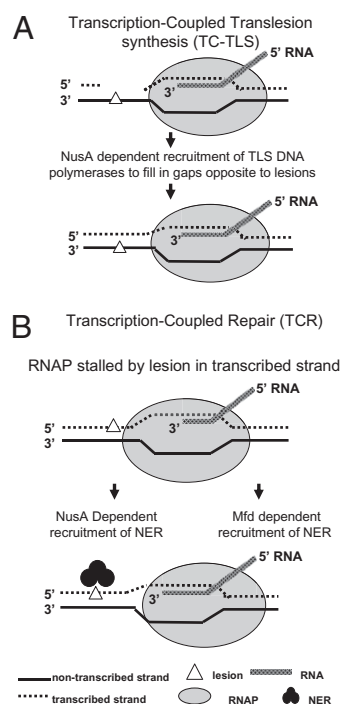


Fig. 6. Models of NusA involvement in two distinct and previously unrecognized pathways: transcription-coupled translesion synthesis (TC-TLS) and an alternative class of transcription-coupled repair. (A) Model of TC-TLS. NusA, associated with elongating RNA polymerases, can recruit TLS polymerases to fill in gaps opposite to lesions in the transcribed strand to allow for the continuation of transcription. (B) An alternative class of TCR, NusA-dependent TCR, where NusA participates in a previously unrecognized branch of the TCR pathway. NusA is capable of recruiting NER to sites of stalled RNAPs to repair DNA lesions on the transcribed strand.

nusA-dependent transcriptional repair of these endogenous lesions through the recruitment of DNA repair and damage tolerance factors to stalled replication forks. If this were the case, NusA-dependent transcriptional recruitment of repair factors in stationary phase might be much more important in helping cells cope with these endogenous lesions because of the absence of replication. This defect in processing endogenously generated DNA damage may be a contributing factor to the reduction of stress-induced mutagenesis, a measure of mutagenesis in nongrowing or very slowly growing cells, observed in a *nusA11* mutant background (9). We proposed that this defect may be a reflection of a deficiency in DNA repair or an inability to recruit DinB for TC-TLS under stressed conditions.

Our model of NusA-TCR complements our previously described model of TC-TLS (8), which proposes that NusA associated with elongating RNAP also recruits TLS polymerases to RNA polymerases stalled at gaps in the transcribed strand that are opposite to a lesion in the nontranscribed strand (Fig. 6). Such gaps could be generated during DNA replication by lesions that cannot be bypassed by the replicative DNA polymerase. Either the resumption of replication at the next Okazaki fragment on the lagging strand or replication restart on the leading strand can generate such a gap, estimated to average ~1,000 ntd in length (52–55). Additionally, such gaps could arise during the *uvr*-dependent processing of two lesions that are very close together but on opposing strands or during the repair of an intrastrand cross-link; in these cases, the gap generated would be much shorter (12–13 ntd) (1). We have shown here that although *E. coli* RNAP is capable of inefficiently bypassing a template strand gap of 1 ntd, it cannot bypass a gap of 14 ntd. Thus, by copying over such lesions in the nontranscribed strand, the TLS DNA polymerase could fill in gaps in the transcribed strand, thereby allowing for the continuation of transcription.

Finally, the fact that plasmids overexpressing *dinB* or *umuDC* partially suppress the temperature sensitivity of a *nusA11* mu-

tant strain, in a manner that requires the catalytic activities of DinB and UmuDC (8), suggests that a key problem cells experience upon losing NusA function is a potentially lethal issue with their DNA. Thus, in addition to transcription termination or antitermination, an important biological role for NusA may be to coordinate DNA repair and damage tolerance systems to resolve problems that arise when transcription is attempted on damaged DNA.

Materials and Methods

Strains and plasmids used in this study are listed in Table S3. DNA damage sensitivity assays, microarray analysis, protein purification, *in vitro* transcription, far-Western blotting, RNAP mutant screening, and live-cell mi-

croscopy are based on published methods. A detailed description of these procedures can be found in *SI Materials and Methods*.

ACKNOWLEDGMENTS. We thank Daniel Jarosz, James Delaney, and John Essigmann (Massachusetts Institute of Technology) for synthesis of the N^2 -furfuryl-dG-containing oligonucleotide, and Laurie Waters for critical reading of the manuscript. This work was supported by National Institutes of Health Grant CA21615 (to G.C.W.), National Institute of Environmental Health Sciences Grant P30 ES002109 (to the MIT Center for Environmental Health Sciences), National Institutes of Health Grant GM38660 (to R.L.), National Institutes of Health Grant DP10D003644, the National Science Foundation's Frontiers in Integrative Biological Research program, and the Howard Hughes Medical Institute (to J.J.C.). C.A.L. was supported by an Undergraduate Biological Science Education Program Award from the Howard Hughes Medical Institute. G.C.W. is an American Cancer Society Research Professor.

- Friedberg EC, et al. (2005) *DNA Repair and Mutagenesis* (Am Soc Microbiol, Washington, DC), 2nd Ed.
- Bohr VA, Smith CA, Okumoto DS, Hanawalt PC (1985) DNA repair in an active gene: Removal of pyrimidine dimers from the DHFR gene of CHO cells is much more efficient than in the genome overall. *Cell* 40:359–369.
- Mellon I, Spivak G, Hanawalt PC (1987) Selective removal of transcription-blocking DNA damage from the transcribed strand of the mammalian DHFR gene. *Cell* 51:241–249.
- Mellon I, Hanawalt PC (1989) Induction of the Escherichia coli lactose operon selectively increases repair of its transcribed DNA strand. *Nature* 342:95–98.
- Park JS, Marr MT, Roberts JW (2002) E. coli transcription repair coupling factor (Mfd protein) rescues arrested complexes by promoting forward translocation. *Cell* 109:757–767.
- Selby CP, Witkin EM, Sancar A (1991) Escherichia coli mfd mutant deficient in "mutation frequency decline" lacks strand-specific repair: *In vitro* complementation with purified coupling factor. *Proc Natl Acad Sci USA* 88:11574–11578.
- Selby CP, Sancar A (1993) Molecular mechanism of transcription-repair coupling. *Science* 260:53–58.
- Cohen SE, Godoy VG, Walker GC (2009) Transcriptional modulator NusA interacts with translesion DNA polymerases in Escherichia coli. *J Bacteriol* 191:665–672.
- Cohen SE, Walker GC (2010) The transcription elongation factor NusA is required for stress-induced mutagenesis in Escherichia coli. *Curr Biol* 20:80–85.
- Jarosz DF, Godoy VG, Delaney JC, Essigmann JM, Walker GC (2006) A single amino acid governs enhanced activity of DinB DNA polymerases on damaged templates. *Nature* 439:225–228.
- Kumari A, et al. (2008) Replication bypass of interstrand cross-link intermediates by Escherichia coli DNA polymerase IV. *J Biol Chem* 283:27433–27437.
- Minko IG, et al. (2008) Replication bypass of the acrolein-mediated deoxyguanine DNA-peptide cross-links by DNA polymerases of the DinB family. *Chem Res Toxicol* 21:1983–1990.
- Yuan B, Cao H, Jiang Y, Hong H, Wang Y (2008) Efficient and accurate bypass of N²-(1-carboxyethyl)-2'-deoxyguanosine by DinB DNA polymerase *in vitro* and *in vivo*. *Proc Natl Acad Sci USA* 105:8679–8684.
- Mooney RA, et al. (2009) Regulator trafficking on bacterial transcription units *in vivo*. *Mol Cell* 33:97–108.
- Chan CL, Landick R (1993) Dissection of the his leader pause site by base substitution reveals a multipartite signal that includes a pause RNA hairpin. *J Mol Biol* 233:25–42.
- Farnham PJ, Greenblatt J, Platt T (1982) Effects of NusA protein on transcription termination in the tryptophan operon of Escherichia coli. *Cell* 29:945–951.
- Greenblatt J, Li J (1981) Interaction of the sigma factor and the nusA gene protein of E. coli with RNA polymerase in the initiation-termination cycle of transcription. *Cell* 24:421–428.
- Landick R, Yanofsky C (1987) Isolation and structural analysis of the Escherichia coli trp leader paused transcription complex. *J Mol Biol* 196:363–377.
- Linn T, Greenblatt J (1992) The NusA and NusG proteins of Escherichia coli increase the *in vitro* readthrough frequency of a transcriptional attenuator preceding the gene for the β subunit of RNA polymerase. *J Biol Chem* 267:1449–1454.
- Liu K, Zhang Y, Severinov K, Das A, Hanna MM (1996) Role of Escherichia coli RNA polymerase α subunit in modulation of pausing, termination and anti-termination by the transcription elongation factor NusA. *EMBO J* 15:150–161.
- Schmidt MC, Chamberlin MJ (1987) nusA protein of Escherichia coli is an efficient transcription termination factor for certain terminator sites. *J Mol Biol* 195:809–818.
- Ha KS, Toulkhonov I, Vassilyev DG, Landick R (2010) The NusA N-terminal domain is necessary and sufficient for enhancement of transcriptional pausing via interaction with the RNA exit channel of RNA polymerase. *J Mol Biol*, in press.
- Cardinale CJ, et al. (2008) Termination factor Rho and its cofactors NusA and NusG silence foreign DNA in E. coli. *Science* 320:935–938.
- Pósfai G, et al. (2006) Emergent properties of reduced-genome Escherichia coli. *Science* 312:1044–1046.
- Jarosz DF, Cohen SE, Delaney JC, Essigmann JM, Walker GC (2009) A DinB variant reveals diverse physiological consequences of incomplete TLS extension by a Y-family DNA polymerase. *Proc Natl Acad Sci USA* 106:21137–21142.
- Wu YH, Franden MA, Hawker JR, Jr, McHenry CS (1984) Monoclonal antibodies specific for the α subunit of the Escherichia coli DNA polymerase III holoenzyme. *J Biol Chem* 259:12117–12122.
- Kim SR, Matsui K, Yamada M, Gruz P, Nohmi T (2001) Roles of chromosomal and episomal dinB genes encoding DNA pol IV in targeted and untargeted mutagenesis in Escherichia coli. *Mol Genet Genomics* 266:207–215.
- Liu J, Doetsch PW (1996) Template strand gap bypass is a general property of prokaryotic RNA polymerases: Implications for elongation mechanisms. *Biochemistry* 35:14999–15008.
- Zhou W, Doetsch PW (1993) Effects of abasic sites and DNA single-strand breaks on prokaryotic RNA polymerases. *Proc Natl Acad Sci USA* 90:6601–6605.
- Butland G, et al. (2005) Interaction network containing conserved and essential protein complexes in Escherichia coli. *Nature* 433:531–537.
- Ona KR, Courcelle CT, Courcelle J (2009) Nucleotide excision repair is a predominant mechanism for processing nitrofurazone-induced DNA damage in Escherichia coli. *J Bacteriol* 191:4959–4965.
- Santangelo TJ, Mooney RA, Landick R, Roberts JW (2003) RNA polymerase mutations that impair conversion to a termination-resistant complex by Q antiterminator proteins. *Genes Dev* 17:1281–1292.
- Vassilyev DG, Vassilyeva MN, Perederina A, Tahirov TH, Artsimovitch I (2007) Structural basis for transcription elongation by bacterial RNA polymerase. *Nature* 448:157–162.
- McCool JD, et al. (2004) Measurement of SOS expression in individual Escherichia coli K-12 cells using fluorescence microscopy. *Mol Microbiol* 53:1343–1357.
- Renzette N, et al. (2005) Localization of RecA in Escherichia coli K-12 using RecA-GFP. *Mol Microbiol* 57:1074–1085.
- Lane WJ, Darst SA (2010) Molecular evolution of multisubunit RNA polymerases: Sequence analysis. *J Mol Biol* 395:671–685.
- Zenkin N, Naryshkina T, Kuznedelov K, Severinov K (2006) The mechanism of DNA replication primer synthesis by RNA polymerase. *Nature* 439:617–620.
- Mah TF, Kuznedelov K, Mushegian A, Severinov K, Greenblatt J (2000) The α subunit of E. coli RNA polymerase activates RNA binding by NusA. *Genes Dev* 14:2664–2675.
- Shankar S, Hatoum A, Roberts JW (2007) A transcription antiterminator constructs a NusA-dependent shield to the emerging transcript. *Mol Cell* 27:914–927.
- Yang X, et al. (2009) The structure of bacterial RNA polymerase in complex with the essential transcription elongation factor NusA. *EMBO Rep* 10:997–1002.
- Ito K, Nakamura Y (1996) Localization of nusA-suppressing amino acid substitutions in the conserved regions of the β' subunit of Escherichia coli RNA polymerase. *Mol Gen Genet* 251:699–706.
- Troelstra C, et al. (1992) ERCC6, a member of a subfamily of putative helicases, is involved in Cockayne's syndrome and preferential repair of active genes. *Cell* 71:939–953.
- Andrews AD, Barrett SF, Yoder FW, Robbins JH (1978) Cockayne's syndrome fibroblasts have increased sensitivity to ultraviolet light but normal rates of unscheduled DNA synthesis. *J Invest Dermatol* 70:237–239.
- George DL, Witkin EM (1974) Slow excision repair in an mfd mutant of Escherichia coli. *Mol Gen Genet* 133:283–291.
- Mei Kwei JS, et al. (2004) Blockage of RNA polymerase II at a cyclobutane pyrimidine dimer and 6-4 photoproduct. *Biochem Biophys Res Commun* 320:1133–1138.
- Donahue BA, Yin S, Taylor JS, Reines D, Hanawalt PC (1994) Transcript cleavage by RNA polymerase II arrested by a cyclobutane pyrimidine dimer in the DNA template. *Proc Natl Acad Sci USA* 91:8502–8506.
- Selby CP, Drapkin R, Reinberg D, Sancar A (1997) RNA polymerase II stalled at a thymine dimer: Footprint and effect on excision repair. *Nucleic Acids Res* 25:787–793.
- Selby CP, Sancar A (1990) Transcription preferentially inhibits nucleotide excision repair of the template DNA strand *in vitro*. *J Biol Chem* 265:21330–21336.
- Pleasant ED, et al. (2010) A comprehensive catalogue of somatic mutations from a human cancer genome. *Nature* 463:191–196.
- Pleasant ED, et al. (2010) A small-cell lung cancer genome with complex signatures of tobacco exposure. *Nature* 463:184–190.
- Lee W, et al. (2010) The mutation spectrum revealed by paired genome sequences from a lung cancer patient. *Nature* 465:473–477.
- Heller RC, Mariani KJ (2006) Replication fork reactivation downstream of a blocked nascent leading strand. *Nature* 439:557–562.
- Iyer VN, Rupp WD (1971) Usefulness of benzoylated naphthoylated DEAE-cellulose to distinguish and fractionate double-stranded DNA bearing different extents of single-stranded regions. *Biochim Biophys Acta* 228:117–126.
- Kornberg A, Baker TA (1992) *DNA Replication* (Freeman, New York).
- Rupp WD, Howard-Flanders P (1968) Discontinuities in the DNA synthesized in an excision-defective strain of Escherichia coli following ultraviolet irradiation. *J Mol Biol* 31:291–304.

Supporting Information

Cohen et al. 10.1073/pnas.1005203107

SI Material and Methods

Bacterial Strains and Plasmids. The strains and plasmids used in this study are listed in Table S3 and were constructed using standard molecular biology techniques. Plasmids were maintained with ampicillin (100 µg/mL) when necessary.

DNA Damage Sensitivity Assays. Independent overnight *E. coli* cultures grown in LB medium were diluted in M9 minimal salts and plated on LB agar containing NFZ, 4-NQO, or MMS. For UV survival assays, cells were plated on LB agar and then irradiated with UV light (0–40 J/m²) by using a G15T8 UV lamp (GE) at 254 nm, then incubated in the dark. A concentrated stock solution of NFZ or 4-NQO was first made in *N,N*-dimethylformamide, stored at –20 °C, and diluted appropriately for each experiment. Percent survival was determined relative to growth in the absence of DNA-damaging agent.

Microarray Analysis. Cultures were grown in Luria–Bertani (LB) medium at 30 °C to exponential phase. RNA samples were prepared from three independent cultures of AB1157 (*nusA*⁺) or AB1157 *nusA11* (SEC164) using a Qiagen RNeasy extraction kit according to the manufacturer's directions, and RNA samples were treated with DNA-free (Ambion) to remove residual DNA according to the manufacturer's instructions. Microarray data collection and analysis were performed as described in refs. 1 and 2. Microarray *.CEL files were combined with *.CEL files from arrays that comprise the M3D compendium (1) [<http://m3d.bu.edu> (E_coli_v3_Build_3)] and RMA-normalized (3) with RMAexpress. Each gene's SD of expression, σ , was calculated across the entire compendium and used to construct the *z*-scale difference between that gene's normalized expression in the *nusA11* strain versus the *nusA*⁺ control:

$$\Delta z_{\text{exp}} = \frac{X_{\text{exp}} - X_{\text{ctl}}}{\sigma}$$

This allowed us to measure each gene's change in expression for a given experiment in units of SD, a form of the *z*-test. For each set of strains in the experiment set, we converted *z* scores to *p* values and chose significantly up- and down-regulated genes by selecting those with a *q* value of <0.05 (false discovery rate) (4).

Protein Purification. NusA and NusA11 proteins were purified from BL21(DE3) pLysS cells containing a His₆-NusA overexpression plasmid (pNusA or pNusA11) (Table S3) by a two-step purification protocol using Ni-NTA and monoQ affinity chromatography. For purification of *E. coli* RNAP BL21(DE3) pLysS cells overexpressing β(β_{His10})αω from pRL4455, a derivative of pRL4930 (5). Cells were lysed by sonication and RNAP purified by polyethyleneimine precipitation followed by ammonium sulfate precipitation, Ni-NTA, and Heparin affinity chromatography.

In Vitro Transcription. DNA and RNA oligonucleotides used to generate transcription substrates are listed in Table S3 and were purified by denaturing PAGE before use. The 14-mer oligonucleotide containing the *N*²-furfuryl-dG adduct was synthesized and purified as described in ref. 6. The nucleic acid templates for in vitro transcription were assembled in reconstitution buffer (RB) [20 mM Tris-HCl (pH 8.0), 40 mM KCl, 5 mM MgCl₂] by heating (NT)DNA and (T)DNA containing a 9-ntd noncomplementary region (bubble) and RNA primer to 75 °C and cooled slowly to 25 °C. Oligonucleotide 6879 (1 µM) is used for (NT)DNA. Oligonucleotides

6987, 6883, and 6896 are used (1 µM each) to generate full-length undamaged strand; 6881, 6883, and 6896 are used to generate 1-ntd gap template; 6897, f-dG, and 6896 are used to generate damaged template; 6897 and 6896 are used to generate 14-ntd gap template. Template strand was ligated with 2,000 units of T4 DNA ligase (NEB) and 1 mM ATP. Reconstitution of TECs was performed by incubating core *E. coli* RNAP (2.5 µM) with the nucleic acid scaffold in RB for 10 min at room temperature. At 37 °C TECs were diluted in RB to contain 50 nM TECs before adding 10 µM UTP and 10 µCi [α-³²P]GTP to label and extend the RNA to position G12. Next, ATP, UTP, and GTP (10 µM each) were added to allow RNAP to elongate to G27. Addition of CTP (10 µM) allows for transcription to continue to the end of the template in the case of full-length, undamaged substrates. Samples were removed at pre-determined times, quenched with an equal volume 2× loading dye [8 M urea, 50 nM EDTA, 90 mM Tris-borate buffer (pH 8.3), 0.02% bromophenol blue, 0.02% xylene cyanol], and analyzed by denaturing 20% polyacrylamide gel electrophoresis. The gel was exposed to a PhosphorImager screen and analyzed using ImageQuant software (GE Healthcare). To map the position of the transcript generated on the *N*²-f-dG template, a C28 marker was made by adding 50 µM dCTP instead of CTP to a reaction with the full-length/undamaged template. Scaffolds to test transcription when *N*²-f-dG is present on the nontranscribed strand are described in Fig. S2 and Table S3. Ligation and reaction conditions were as above.

Far-Western Blotting. An equivalent number of BL21 cells expressing UvrA from pMP47 or containing the empty vector (pET11) were lysed by boiling in SDS-loading dye and lysates were separated by SDS/PAGE (4–12%), transferred to a poly(vinylidene difluoride) membrane, and probed with purified recombinant NusA (2 µM final concentration). Anti-NusA Western blotting was then performed as described in ref. 7. Monoclonal anti-NusA antibody was obtained from Neoclone.

RNA Polymerase Mutant Screen. Mutagenized libraries of pRL706 (8) transformed into AB1157 were grown in LB medium supplemented with ampicillin induced with 1 mM IPTG. Under induced conditions, it has been estimated that ~85%–90% of cellular RNAPs have incorporated the plasmid-encoded His₆-tagged subunit (8). Cultures were diluted in M9 minimal salts and 10-fold dilutions stamped onto LB agar containing ampicillin and either 0 or 10 µM NFZ with a 96-well pin replicator. Plates were incubated at 37 °C and scored for NFZ sensitivity or resistance the next day. All candidates were isolated and repeated for confirmation. Plasmids from confirmed clones were isolated and sequenced. Of ~800 mutants screened, 6 NFZ^R mutants and 23 NFZ^S mutants were isolated.

Live-Cell Microscopy. Live-cell microscopy was performed as described in refs. 9 and 10. Aliquots of cells were stained with the membrane dye FM4-64 (240 ng/mL to 1 µg/mL; Molecular Probes). Cells were then placed on a pad of 4% low melt agarose in a solution of M9 minimal salts and covered with a coverslip. The following Chroma filter sets were used: 41002b (TRITC) for FM4-64 and 41012 for GFP. Images were acquired using a Nikon E800 microscope with a charge-coupled device camera (Hamamatsu model C4742-95) and OpenLab software (Improvision). Images were colored in OpenLab and then transferred to Photoshop (Adobe) for figure assembly.

1. Faith JJ, et al. (2007) Large-scale mapping and validation of *Escherichia coli* transcriptional regulation from a compendium of expression profiles. *PLoS Biol* 5:e8.
2. Kohanski MA, Dwyer DJ, Hayete B, Lawrence CA, Collins JJ (2007) A common mechanism of cellular death induced by bactericidal antibiotics. *Cell* 130:797–810.
3. Bolstad BM, Irizarry RA, Astrand M, Speed TP (2003) A comparison of normalization methods for high density oligonucleotide array data based on variance and bias. *Bioinformatics* 19:185–193.
4. Storey JD, Tibshirani R (2003) Statistical significance for genomewide studies. *Proc Natl Acad Sci USA* 100:9440–9445.
5. Touloukhonov I, Zhang J, Palangat M, Landick R (2007) A central role of the RNA polymerase trigger loop in active-site rearrangement during transcriptional pausing. *Mol Cell* 27:406–419.
6. Jarosz DF, Godoy VG, Delaney JC, Essigmann JM, Walker GC (2006) A single amino acid governs enhanced activity of DinB DNA polymerases on damaged templates. *Nature* 439:225–228.
7. Beuning PJ, Sawicka D, Barsky D, Walker GC (2006) Two processivity clamp interactions differentially alter the dual activities of UmuC. *Mol Microbiol* 59:460–474.
8. Santangelo TJ, Mooney RA, Landick R, Roberts JW (2003) RNA polymerase mutations that impair conversion to a termination-resistant complex by Q antiterminator proteins. *Genes Dev* 17:1281–1292.
9. Smith BT, Grossman AD, Walker GC (2001) Visualization of mismatch repair in bacterial cells. *Mol Cell* 8:1197–1206.
10. Smith BT, Grossman AD, Walker GC (2002) Localization of UvrA and effect of DNA damage on the chromosome of *Bacillus subtilis*. *J Bacteriol* 184:488–493.

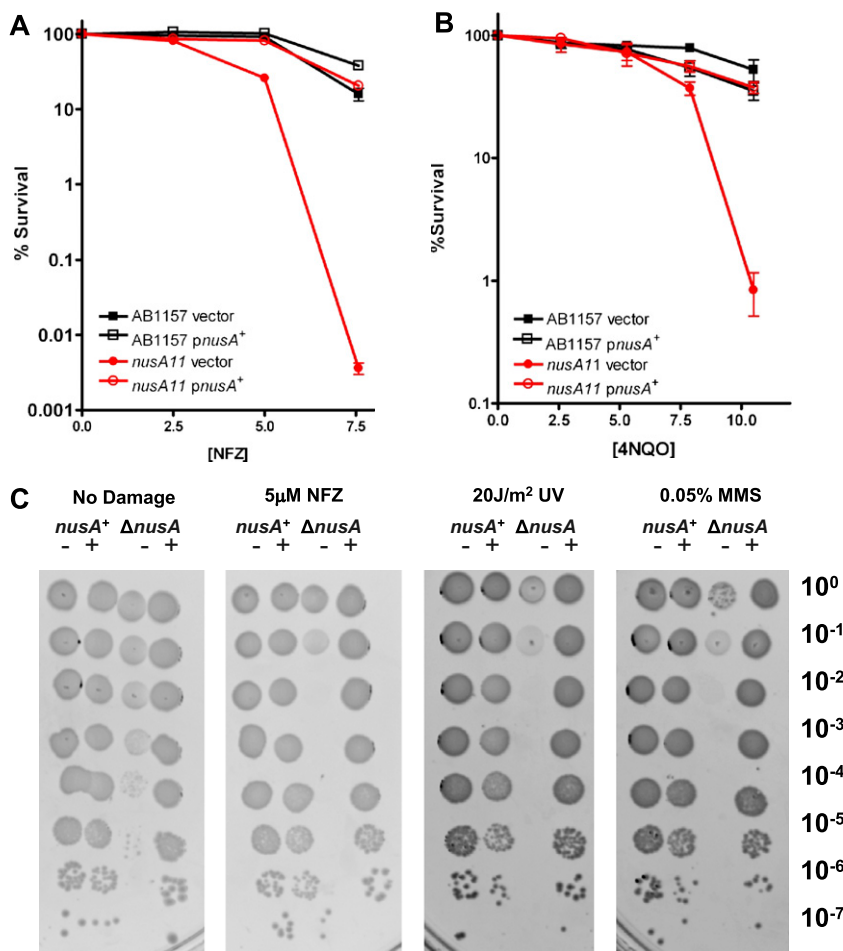


Fig. 51. (A and B) Sensitivity of *nusA11* mutant strains to NFZ (μM) (A) and 4-NQO (μM) (B) can be complemented *in trans* at 30 °C in AB1157. pBR322 is used as an empty vector and pNAG2010 is *pnuA*⁺, and are described in Table S2. SD determined from at least three independent cultures. (C) Sensitivity of $\Delta nusA$ strains to NFZ, UV, and MMS can be complemented *in trans*. Growth of 10-fold serial dilutions, labeled to the left, of designated strains is depicted in photograph. *nusA*⁺ represents MDS42 and $\Delta nusA$ represents MDS42 $\Delta nusA$. -, empty vector (pBR322); +, *pnuA*⁺ (pNAG2010).

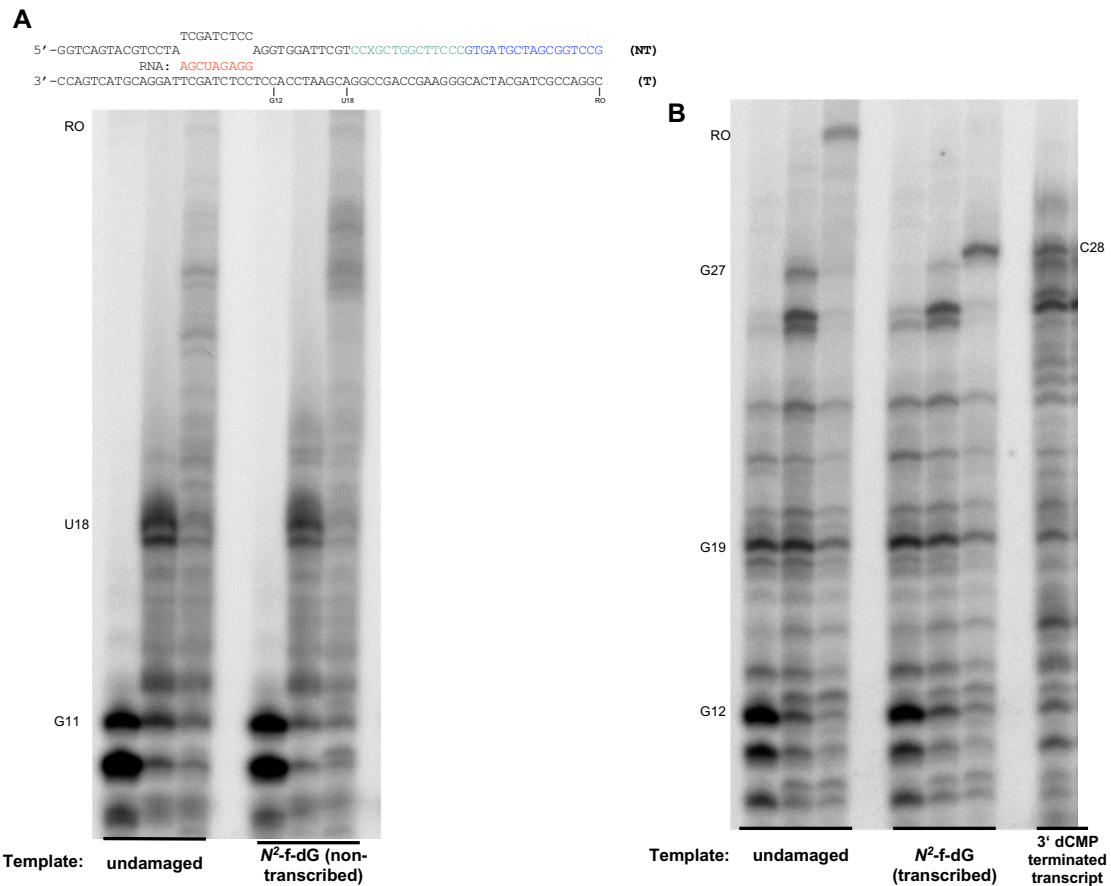


Fig. S2. (A) *N*²-f-dG on the nontranscribed strand does not block transcription. Schematic of experimental design: three oligonucleotides, one containing the *N*²-f-dG lesion or an undamaged proxy, are ligated together to generate the nontranscribed strand (NT) using the transcribed strand (6910) (T) as a scaffold. "X" indicates a site of *N*²-furfuryl-dG lesion or proxy dG. A 9-ntd noncomplementary region between the (T)DNA and (NT)DNA allows for the annealing of an RNA primer (shown in red) to initiate transcription. Oligonucleotides 6920 (black), 6883 or f-dG (green), and 6930 (blue) are used to generate the nontranscribed strand. For each nucleic acid scaffold, undamaged or *N*²-f-dG (in the NT strand), purified RNAP, ATP, and [α -³²P]GTP are added to allow for radiolabel incorporation into the RNA transcript and extend to G11 (first lane). The addition of excess cold ATP, UTP, and GTP extends the transcription elongation complex (TEC) to U18 position, 5 nucleotides before the *N*²-f-dG lesion (second lane). Addition of CTP allows for the visualization of the run-off transcript (third lane; band labeled RO). All reactions represent 5-min time points after addition of nucleotide. (B) For nucleic acid templates labeled undamaged and *N*²-f-dG (transcribed) in vitro transcription reactions were carried out as in Fig. 3. The first lane represents the migration of the transcript generated in the presence of radiolabeled GTP, UTP, and limiting ATP. The second lane represents the migration of the transcript generated when excess GTP, UTP, and ATP are added generating a G27 transcript marker. The third lane represents the migration of the transcript generated after the addition of CTP, allowing RNAP to transcribe through the template generating the complete transcript. All samples in this figure were removed 1 min after addition of nucleotide(s). The migration of the run-off transcript generated using the full-length/undamaged template when all NTPs are added is labeled RO. The final lane represents the migration of a C28 marker generated by the addition of dCTP to a reaction using the full-length template. These results demonstrate that the *N*²-f-dG lesion stalls transcription four nucleotides before the site of the lesion.

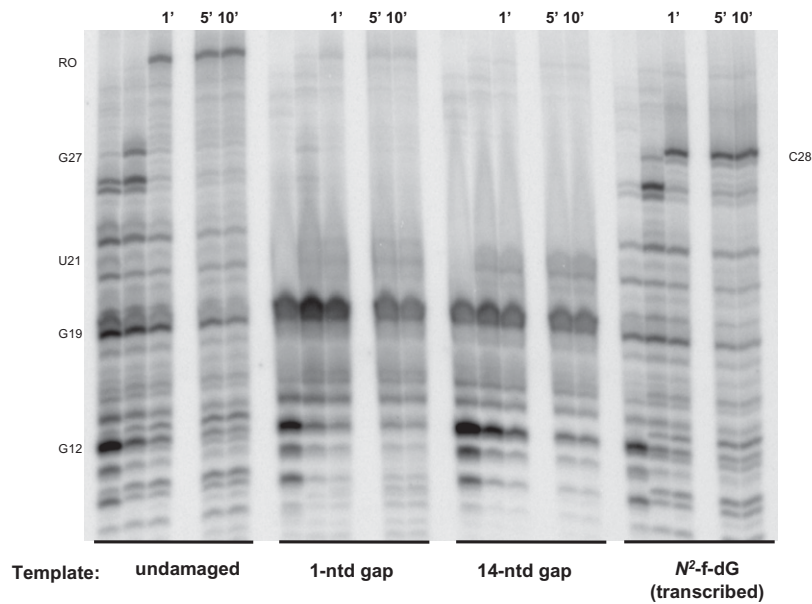


Fig. 53. In vitro transcription reactions were performed as in Fig. 3, except samples were removed 1, 5, and 10 min after addition of CTP. For each template, the first three lanes are the same as those shown in Fig. 3B, with the last of these three lanes representing the product generated 1 min after addition of CTP, noted as 1' above. An empty lane separates the 1' time point and the products generated 5 (5') and 10 (10') minutes after addition of CTP, as labeled above. These results demonstrate that even with prolonged incubation time, *E. coli* RNAP cannot bypass a template strand gap of 14-ntd or the N^2 -f-dG lesion. Nonspecific higher migrating bands are observed in reactions using 14-ntd and N^2 -f-dG templates as these bands are observed before all nucleotides are added to the reaction.

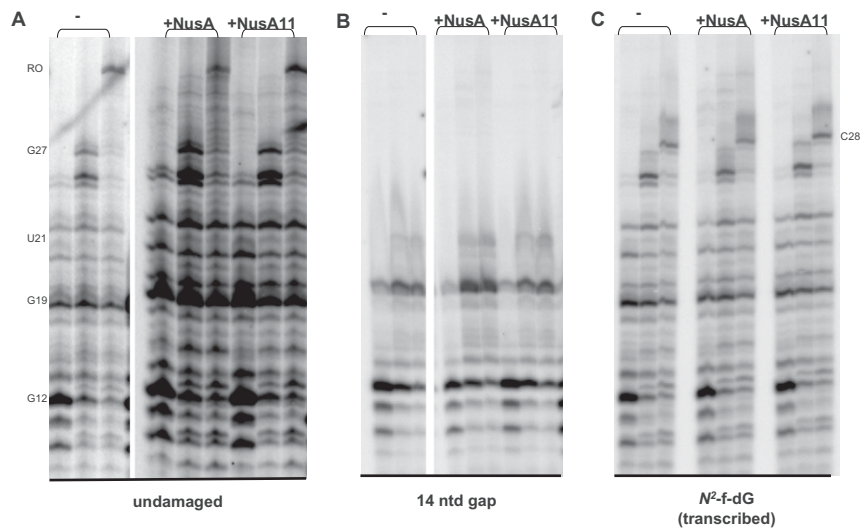


Fig. 54. Addition of purified NusA or NusA11 to in vitro transcription reactions of full-length/undamaged template (A), 14-ntd gapped template (B), or N^2 -f-dG containing template (C). Lanes labeled "-" were performed identically as those done in Fig. 3B. The first lanes represent products formed in the presence of radiolabeled GTP, UTP, and limiting ATP, the addition of excess GTP, UTP, and ATP to lane two and the addition of CTP to lane 3. Lanes labeled +NusA represent reactions performed in the presence of 100 nM purified NusA or NusA11 for lanes labeled +NusA11.

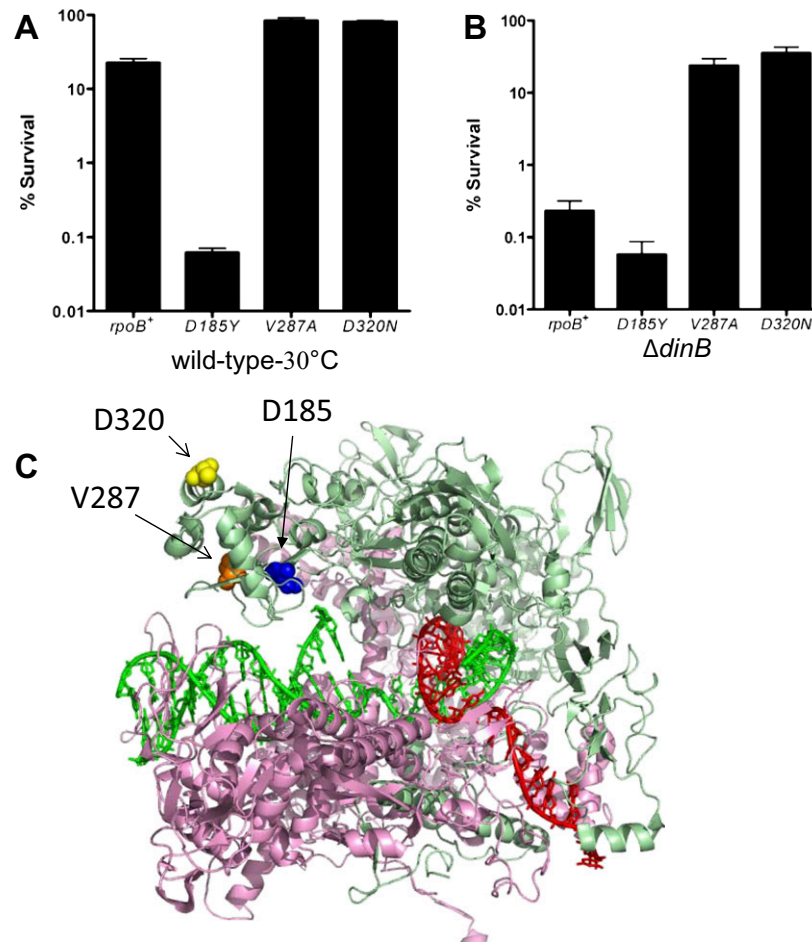


Fig. 55. (A) Percent survival of *rpoB* mutants expressed in AB1157 to 12.5 μ M NFZ at 30 °C. A higher dose of NFZ is used compared with experiments done at 37 °C to observe sensitivity of strains expressing *rpoB*⁺. In this and all graphs in this figure, error bars represent the SD determined from at least three independent cultures. (B) Sensitivity of *rpoB* mutants expressed in a Δ *dinB* background to 10 μ M NFZ at 37 °C. (C) Residues of *rpoB* D185 (blue), V287 (orange), and D320 (yellow) mapped on to the structure of *T. thermophilus* RNAP elongation complex (2O5I). β catalytic subunit shown in pale green, β' in pink, DNA in green, and RNA in red. V287 and D320 are located in a lineage-specific sequence insertion in the lobe domain of *E. coli* RNAP, and V287 is not conserved between *E. coli* and *T. thermophilus*. The residue highlighted in orange is the residue of *T. thermophilus* that is positioned closest to V287 of *E. coli*. The crystal structure predicts that when RNAP stalls at the -4 position relative to the N²-f-dG lesion in the transcribed strand, the N²-f-dG adduct would be located in the minor groove of the dsDNA ahead of the transcription bubble.

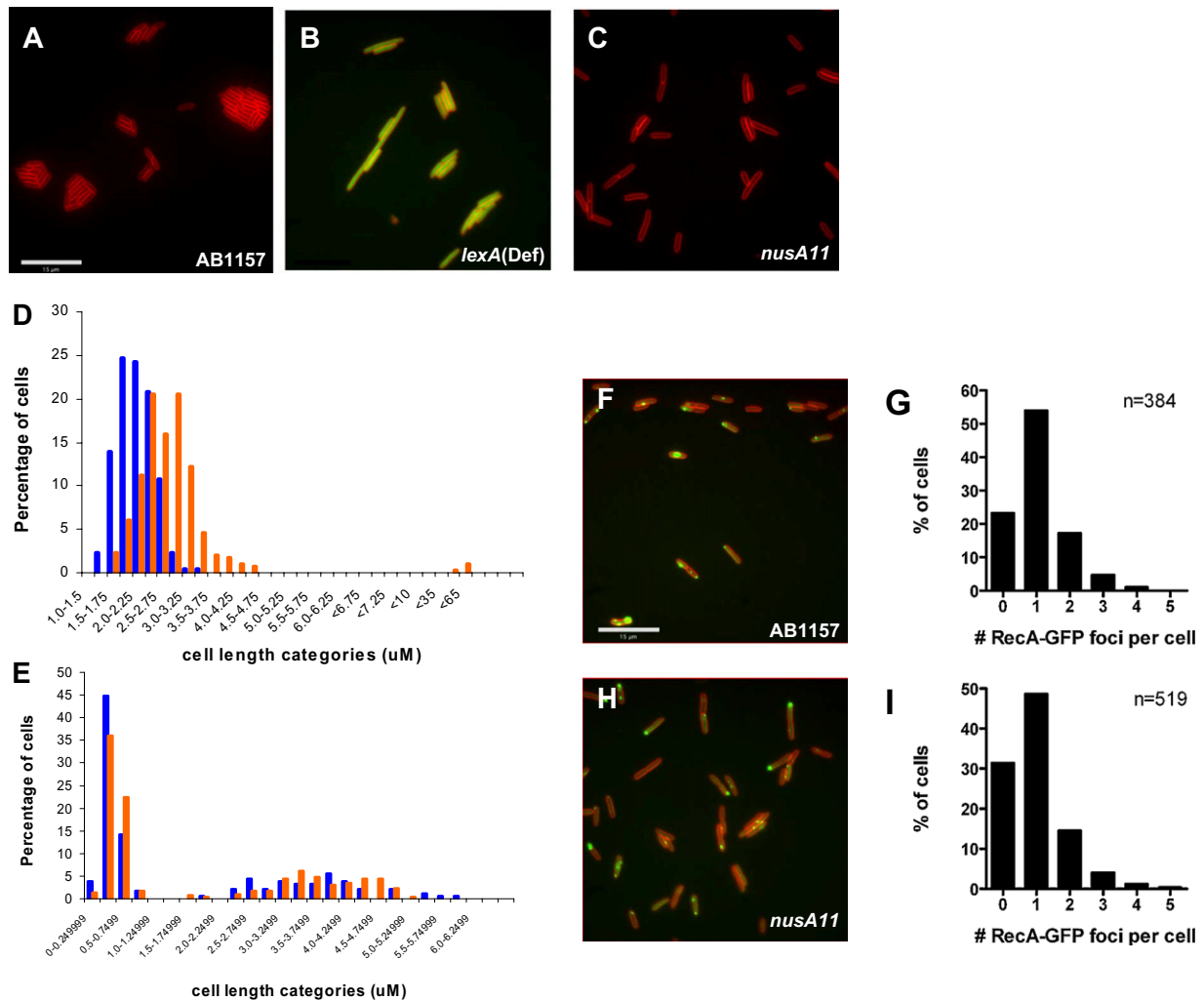


Fig. S6. SOS induction and RecA-GFP foci of exponentially growing cells. (A–C) SOS induction of exponentially growing cells. Representative micrographs of wild-type (AB1157) (SEC677) (A), *lexA(Def)* (SEC678) (B), and *nusA11* (SEC679) (C) cells during exponential growth ($OD_{600} \sim 0.3$). These analyses demonstrate that $\sim 0.2\%$ of wild-type cells are induced for the SOS response ($n = 602$) compared with 100% of *lexA(Def)* ($n = 44$) and 0.8% of *nusA11* ($n = 453$) cells. Cell outlines (red) were visualized with the vital membrane stain FM4-64, and SOS induction was monitored from P_{SUA} -GFP fusion (green). (D) Cell length distributions of stationary-phase wild type/AB1157 (blue) and *nusA11* (orange) show that *nusA11* strains are elongated compared with wild type. (E) Cell length distributions of exponentially growing wild-type/AB1157 (blue) and *nusA11* (orange) cells. (F–I) RecA-GFP foci in exponentially growing cells: Representative micrographs of AB1157 (F) and *nusA11* (H) strains during exponential growth ($OD_{600} \sim 0.3$), and distribution of RecA-GFP foci in *nusA*⁺ (G) and *nusA11* (I) cells. Cell outlines (red) were visualized with the vital membrane stain FM4-64, and RecA-GFP foci are shown in green. All experiments in this figure were performed at the permissive temperature, 30 °C.

Other Supporting Information Files

[Table S1 \(DOC\)](#)

[Table S2 \(DOC\)](#)

[Table S3 \(DOC\)](#)